Feasibility of a Radar Altimeter for an Unmanned Aerial Vehicle Cruising in the Mars' Atmosphere

Sho Yonemura, Atsushi Tomiki, Tomoaki Toda, and Takehiko Kobayashi

***Abstract*— The Japan Aerospace Exploration Agency has planned a Mars exploration using an unmanned aerial vehicle (UAV) ejected from a Mars orbiter for observing the residual magnetic fields near the surfaced and the exposed strata of Mars. An altimeter is indispensable to achieve the mission, which must be miniature and light weight to be equipped on the UAV flying in the thin atmosphere of Mars. For this purpose, we have been developing an FM-CW radar for its accepted merits: easier signal processing and lower power consumption than a pulse radar. Tentative specifications and construction of the altimeter were examined. Normalized radar cross section (RCS) of the Mars' surface, previously unknown, was estimated ranging between -20 and 0 dB from the past radar observation of the earth and the moon. Preliminary signal-to-noise ratio estimation based on the radar equation revealed that the altitude can be measured in the worst case (the normalized RCS = -20 dB) at an altitude of 10 km (the maximum altitude to cruise). This paper presents the feasibility study of the radar altimeter and the results of ranging experiments with use of a breadboard model.**

***Index Terms*—radar altimeter, planet exploration, Mars, UAV**

I. Introduction

THE Japan Aerospace Exploration Agency (JAXA) has planned a Mars exploration, using a Mars orbiter, a rover, and a light unmanned aerial vehicle (UAV) around 2020 [1, 2]. The light UAV has been proposed, which will be ejected from the orbiter for observing the residual magnetic fields near the surface and the exposed strata of Mars, as shown in Fig. 1. This mission cannot be carried out with a rover or an orbiter-borne remote sensor. Since the atmospheric pressure of Mars is approximately a hundredth of that of the earth, an obtainable lifting force of the UAV is significantly smaller than on the earth. Therefore it should have large wings and be lightweight. Weight of onboard equipment and its consumption of electric power also should be minimized.

Manuscript received February 7, 2014.

S. Yonemura and T. Kobayashi are with Tokyo Denki University, Adachi-ku, Tokyo 120-8551, Japan (phone: +81-3-5284-5518; fax: +81-3-5284-5518; e-mail: yonemura@grace.c.dendai.ac.jp, koba@c.dendai.ac.jp).

A. Tomiki and T. Toda are with Institute of Space and Astronautical Science, Japan Aerospace Exploration Agency, Sagamihara-shi, Kanagawa 252-5210, Japan (e-mail: tomiki@isas.jaxa.jp, toda@isas.jaxa.jp).

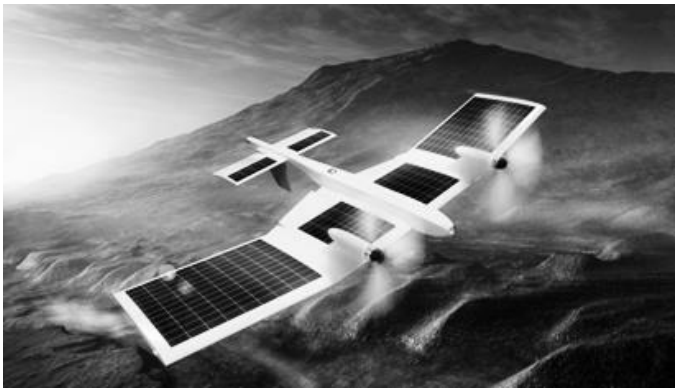

Fig. 1. Artist's concept of a UAV cruising in the Mars' atmosphere.

An altimeter is indispensable for the mission. A conventional laser altimeter used for past planetary exploration is too heavy (*e.g.* 3.7 kg) to apply to this particular light weight UAV. A pulse radar is also unsuitable due to its high power consumption. This present paper examines the feasibility of a frequency-modulated continuous-wave (FM-CW) radar because of its accepted merits: easier signal processing and lower power consumption than a pulse radar.

II. Requirements and a Proposed Solution – FM-CW Radar

The UAV will be folded up to store in a capsule, and be ejected from a Mars orbiter. The capsule will be opened at a height of approximately 10 km and the UAV will start cruising until the battery is drained, and then crash to the Mars surface. It will cruise at altitudes from 0.2 to 10 km, among which the observation is scheduled at altitudes from 1 to 3 km. The requirements for this altimeter are listed in TABLE I. The altitude resolution should be less than 100 m during non-observation periods and 10 m during observation. At present, between 100 and 200 grams is allocated to the altimeter within an UAV weighing approximately 4.2 kg. Power consumption should be less than 1 W. To meet these requirements, we propose an altimeter consisting of an FM-CW radar transceiver and a signal processor, shown in Fig. 2. A radio-frequency (RF) power amplifier of FM-CW radars is more power efficient than that of pulse radars. Furthermore, the power consumption of an analog-to-digital converter (ADC) increases approximately in proportion to its sampling rate. The

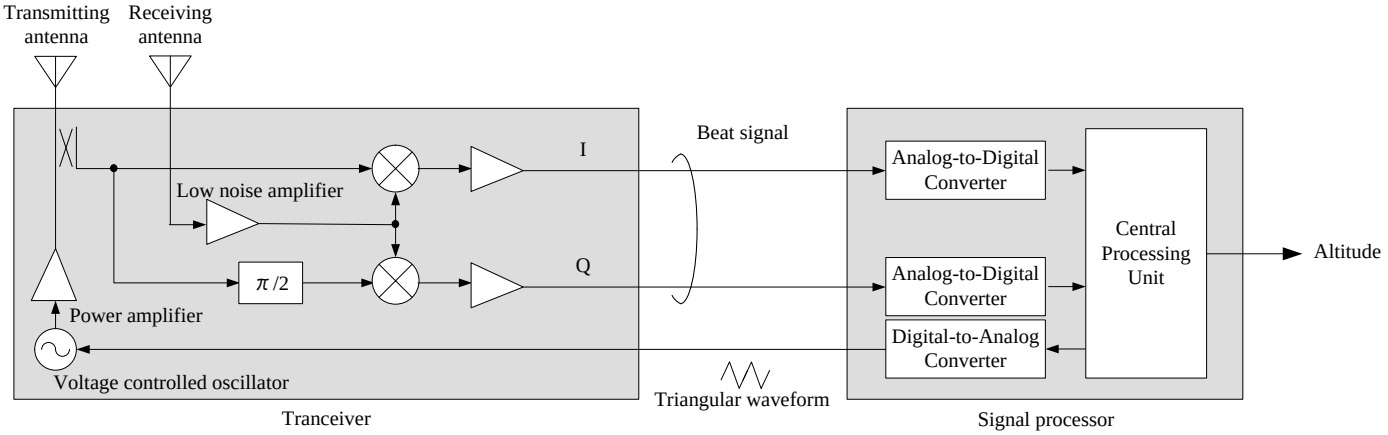

Fig. 2. System configuration of FM-CW radar altimeter.

TABLE I
REQUIREMENTS FOR AN ONBOARD ALTIMETER

Weight	< 200 g
Power consumption	< 1 W
Altitude resolution	< 10 m (during observation) < 100 m (otherwise)
Measurable altitude	200 m to 10 km (observation: 1 to 3 km)
Refresh rate	1 time / second

sampling rate for FM-CW radars is lower than that for pulse radars because of lower intermediate frequency.

The signal processing unit comprises an ADC, a digital-to-analog converter (DAC), and a microprocessor. A voltage-controlled oscillator (VCO) in the transceiver is driven by a triangular waveform generated with the DAC. A beat signal generated with transmitted and received signals is input to the ADC, and the microprocessor thereupon calculates the altitude with use of fast Fourier transformation (FFT). A carrier frequency of 24.15 GHz at Ka band was selected for operation in consideration of the weight of antennas for transmission and reception and international and domestic frequency allocation for radars.

III. BASIC PRINCIPLE OF FM-CW RADAR

The transmitting signal (center frequency = f_0) is frequency-modulated by triangular waveform. Then the frequency gap (beat frequency) between transmitted and received signal appears because the transmitting signal frequency changes during the round-trip of the transmitted signal, as shown in Fig. 3 (a), by assuming a radial velocity v = 0.

The rate of frequency change $\dot{f}$ is,

$$\dot{f} = \frac{\Delta f}{1/2f_m} = 2f_m \Delta f, \qquad (1)$$

where Δf is the frequency excursion and f_m is the frequency of the triangular waveform. The beat frequency f_b is given by

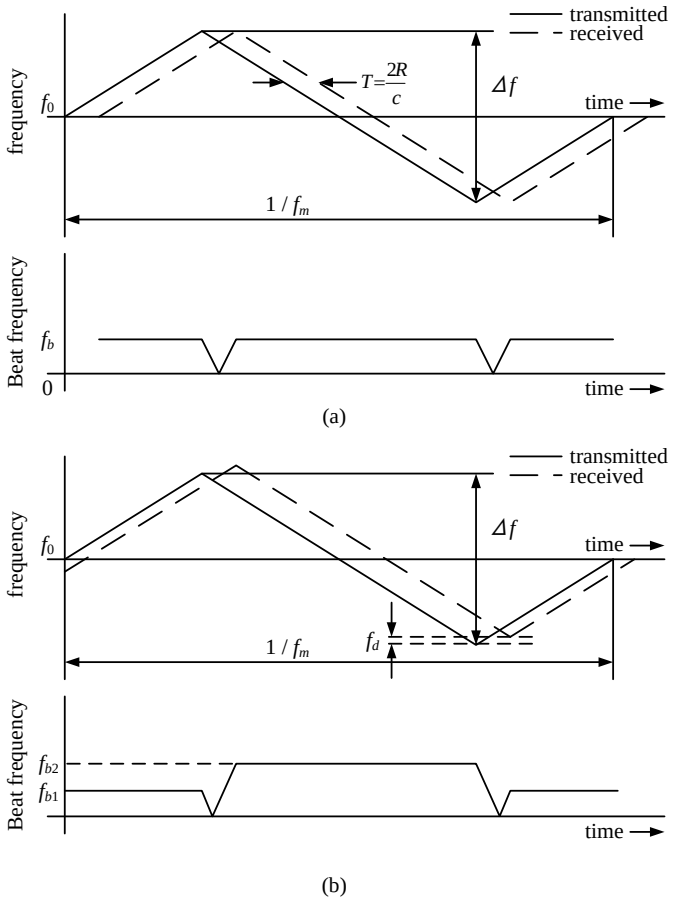

Fig. 3. Transmitted and received frequencies and corresponding beat frequency : with (a) no Doppler shift and (b) a positive Doppler shift (the target is assumed to be approaching the radar).

$$f_b = T\dot{f} = \frac{2R}{c}\dot{f}, \qquad (2)$$

where T is the round-trip time of the RF signal, R is the range of the target, and c is the velocity of light = 3.0×10^8 m/s. Equating Eqs. (1) and (2) and solving for R yields

$$R = \frac{cf_b}{4f_m \Delta f}. \qquad (3)$$

When a radial velocity $v \neq 0$, the received signal is shifted up or down in frequency by the Doppler effect, as shown in Fig. 3 (b), where f_d is the Doppler frequency shift, f_{b1} and f_{b2} are the beat frequencies on the increasing and decreasing portion of the received signal, respectively:

$$\begin{cases} f_{b1} = f_b - f_d & \text{(4a)} \\ f_{b2} = f_b + f_d & \text{(4b)} \end{cases} .$$

The average beat frequency f_b is therefore obtained by

$$f_b = \frac{f_{b1} + f_{b2}}{2} . \quad (5)$$

The Doppler frequency shift f_d is given by

$$f_d = \frac{2vf_0}{c} = \frac{f_{b1} - f_{b2}}{2} . \quad (6)$$

As discussed in the next section, $f_b > f_d$ can be presumed in this radar altimeter.

IV. Feasibility of the FM-CW Altimeter

A. Power Consumption and Modulation Speed

The power consumption of an ADC (ADC7671, Analog Devices Inc.) was measured as shown in Fig. 4. To maintain the power consumption below 100 mW, the sampling rate should be less than 400 kS/s, as shown in Fig. 4, and hence the highest beat frequency should not exceed 200 kHz. The beat frequency depends on the rate of the change of the transmitting signal f_m. On the assumption that the frequency sensitivity against the input voltage of the VCO = 22 MHz/V, and the output voltage of the DAC = 0 to 3.3 V (thus the bandwidth of transmitting signal Δf = 72.6 MHz), the relationship between the frequency of the triangular waveform f_m and the maximum beat frequency f_b was calculated when R = 3 and 10 km by using Eq. (3), as shown in Fig. 5. The maximum beat frequency of 200 kHz is shown by a horizontal broken line in this graph. To measure an altitude of 3 or 10 km, the value of f_m should be less than 68.8 or 20.0 Hz, respectively, as depicted in Fig. 5.

B. Resolution of Altitude

The altitude resolution depends on the maximum beat frequency f_b, the sampling rate of the beat signal f_s, and the number of FFT points N. The altitude resolution ΔR is given by

$$\Delta R = (\text{altitude per unit beat frequency}) \times (\text{frequency resolution}) = \frac{r}{f_b} \cdot \frac{f_s}{N} . \quad (7)$$

Substitution of Eq. (3) into Eq. (7) yields

$$\Delta R = \frac{c}{4 f_m \Delta f} \cdot \frac{f_s}{N} . \quad (8)$$

This relationship between the altitude resolution ΔR and the number of FFT points N is depicted in Fig. 6, assuming f_s = 400 kS/s and Δf = 72.6 MHz. It revealed that $N \geq 1024$ was needed to achieve a resolution of 10 m when f_m = 66.7 Hz (*i.e.* during the observation). This size of FFT and other relevant processing

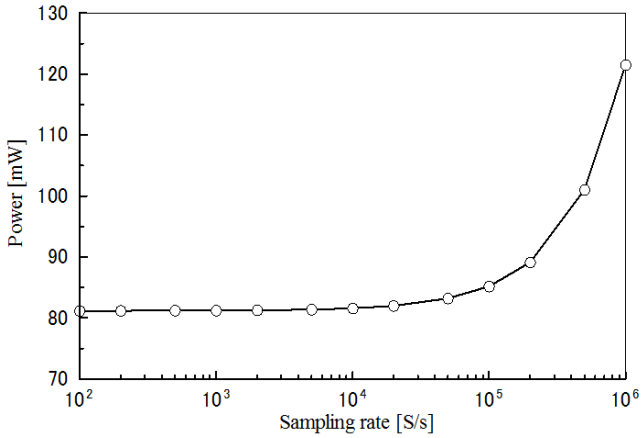

Fig. 4. Relationship between sampling rate and power consumption of an ADC (ADC7671, Analog Devises Inc.).

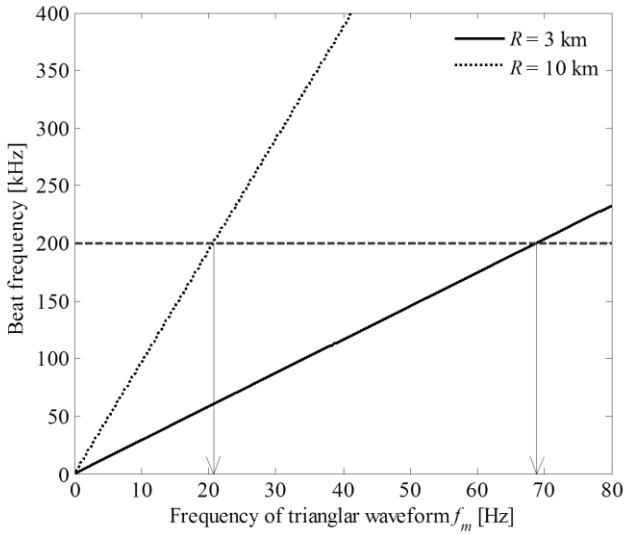

Fig. 5. Relationship between the frequency of triangular waveform and the beat frequency.

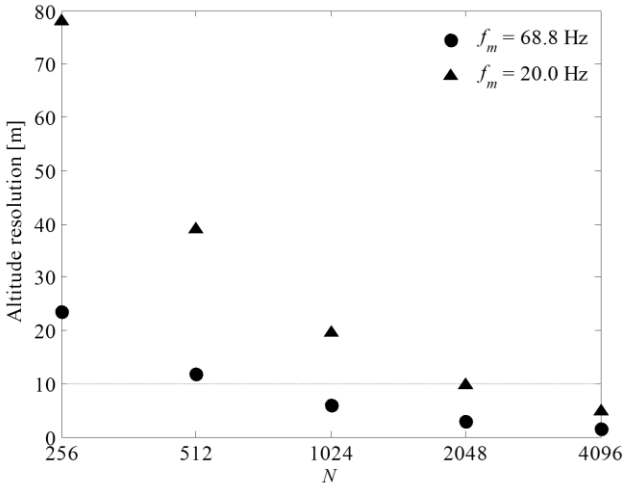

Fig. 6. The relationship between FFT points and the altitude resolution.

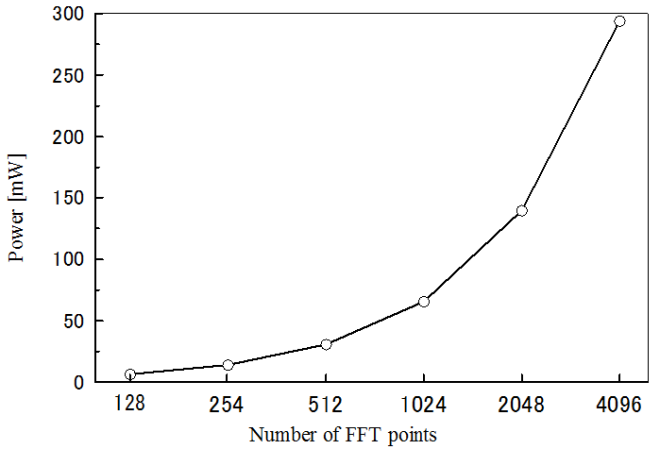

Fig. 7. Relationship between FFT points and power consumption of a microprocessor (LPC2388,. NXP Semiconductors Inc.).

can be readily achieved by using an inexpensive, off-the-shelf microprocessor. The measured power consumption of a microprocessor (LPC2388, NXP Semiconductors Inc.) calculating FFT is depicted in Fig. 7, where the power consumption is reasonably low (65 mW) when $N = 1024$.

C. Probability of False Estimation of f_b

The beat frequency is estimated by applying FFT to the beat signal and detecting the peak of the spectrum. The precision of peak detection depends on signal to noise ratio (SNR) at the radar receiver. The relationship between SNR and the probability of false estimation of f_b was simulated. The simulation was carried out in baseband domain (not in radio frequency domain), as shown in Fig. 8. The beat frequency was 10 kHz and the number of FFT point was 1024. The result is shown in Fig. 9.

The UAV will cruise for 30 minutes and the data is refreshed 1 time per second. Therefore the number of all data is 1800. Hence the probability of false estimation should be less than 10^{-4}, and SNR should exceed 6 dB, from Fig. 9.

D. Estimation of Radar Reflectivity of the Mars' Surface

The SNR at the radar receiver is given by a radar equation:

$$\mathrm{SNR}=\frac{P_t G^2 \sigma \lambda^2}{(4\pi)^3 R^4 L_s k T B F_n}\ , \qquad (9)$$

where

P_t [W] : transmitting power
G: antenna gain
σ [m^2] : radar cross section of a target
λ [m] : wavelength
R [m] : range
L_s: feeder loss
k : the Boltzmann constant(= 1.38 × 10^{-23} J/K)
T [K]: temperature
B [Hz]: bandwidth
F_n: noise figure of the receiver

and

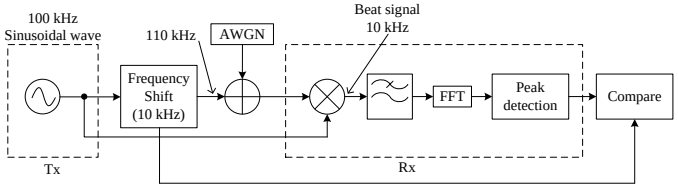

Fig. 8. A baseband simulation model.

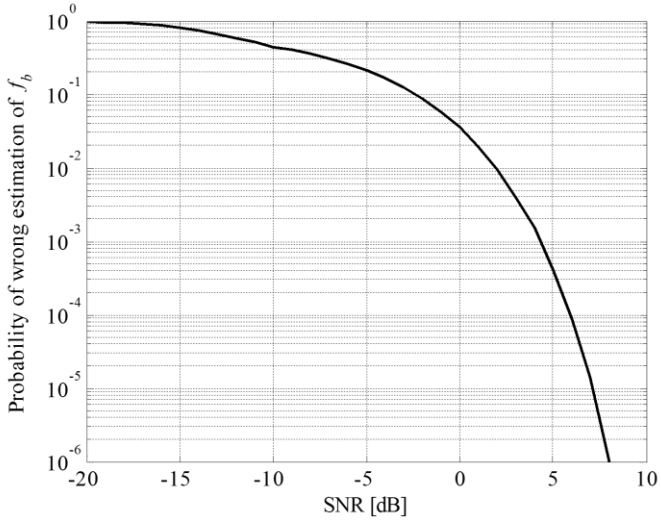

Fig. 9. Relationship between the SNR and probability of false estimation of f_b.

$$\sigma = \sigma^0 \times \text{illuminating area} = \sigma^0 \cdot \frac{\pi R^2}{1.33^2} \tan^2\left(\frac{\Phi}{2}\right)\ , \qquad (10)$$

where Φ is the half-power beamwidth of the antenna and σ^0 is called normalized radar cross section, which is dimensionless and represents the radar reflectivity of an extended target over the radar illuminating area.

Since no data of σ^0 measured on the Mars' surface are available, we have estimated the σ^0 from those of the earth [3] and the moon [4]. Figure 10 shows dependence of σ^0 on the incidence angle measured for three categories of roughness of the earth's surface at Ka-band. When the surface becomes rough, the dependence on the incident angle decreases, as shown in Fig. 10. Since the Mars' surface is significantly rough, the dependence is expected to be small. Figure 11 depicts dependence of the σ^0 of the lunar surface on the incidence angle measured with three different wavelengths. As the wavelength becomes shorter, the effective surface roughness relatively increases, and hence the dependence of the σ^0 on the incident angle decreases. Based on these data, the normalized radar cross sections of the Mars' surface are estimated ranging from -20 to -5 dB within the incidence angle between 3° and 75, as shown by a chained line in Fig. 11.

Major parameters of the proposed radar altimeter are listed in TABLE II. The transmitting power and the antenna gain are limited respectively by the power consumption and the weight requirements. Figure 12 shows the relationship between the altitude and the SNR for various normalized radar cross section

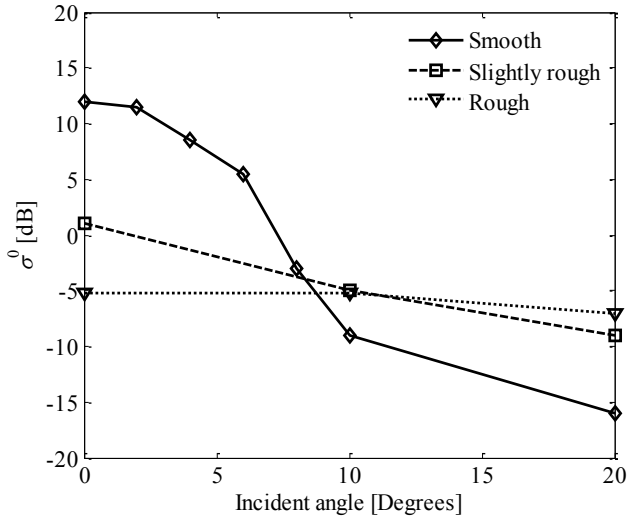

Fig. 10. Normalized radar cross section measured at Ka band on the earth [3].

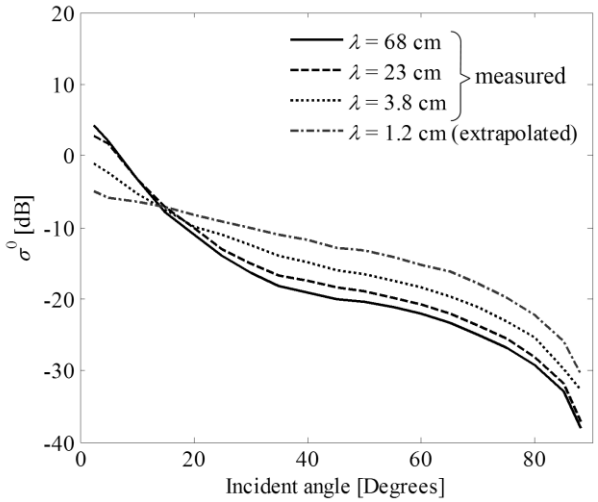

Fig. 11. Normalized radar cross section measured at three different wavelengths on the moon [4] and that extraporated at Ka band.

TABLE II
MAJOR PARAMETERS OF THE RADAR ALTIMETER

Transmitting power	P_t	23	dBm
Antenna gain	G	32	dBi
Wavelength	λ	12.4	mm
Feeder loss	L_s	1	dB
Temperature	T	210	K
Bandwidth	B	200	kHz
Noise figure	F_n	6	dB
Beamwidth	Φ	5.1	Degrees

between –20 to 0 dB with use of Eq. (9) and based on the parameters given in TABLE II. The dotted horizontal line in Fig.12 presents a minimum SNR of 6 dB required for reliable operation. The calculation revealed that the altitude can be measured for a σ^0 of -20 dB even in the severest condition at an altitude of 10 km.

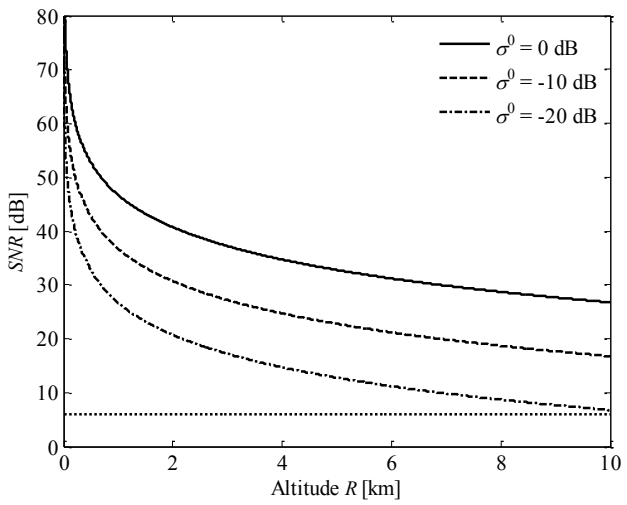

Fig. 12. Relationship between the altitude R and the SNR.

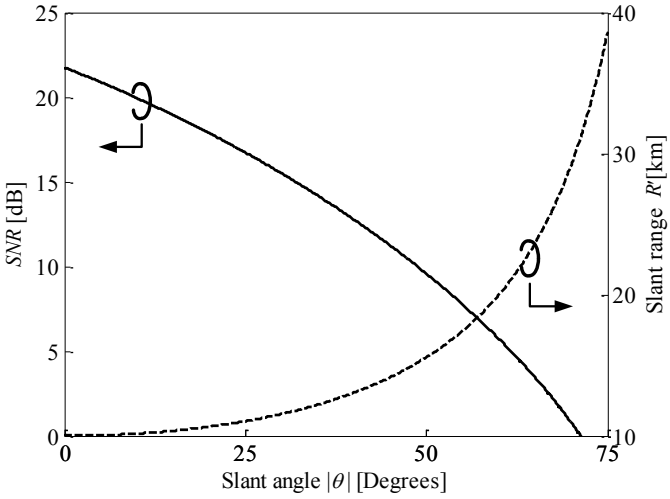

Fig. 13. Relationship between the slant angle θ and the SNR.

E. Other Considerations

Since gusts of wind often blow on Mars, the attitude of the UAV would fluctuate and the radar slants from the straight down direction. Figure 13 presents the relationship between slanting angle θ ($|\theta| < 75°$) and SNR, calculated on the assumption that the altitude = 10 km with use of the data of σ^0 given by the chained curve in Fig. 11. The SNR exceeding 6 dB is maintained for $|\theta| < 60°$. Figure 13 also depicts the relationship between θ and slant range R' ($R' = R \sec \theta$) when R = 10 km, which indicates that the information of the slanting angle (or the attitude of the UAV) is needed to estimate the altitude correctly. An attitude sensing system will be equipped on the UAV [5].

As mentioned in Section III, a Doppler frequency shift is imposed on the received beat frequency, when a radial velocity $\neq 0$. If the aircraft cruises horizontally, but its pitch angle $\psi \neq 0$, a radial velocity v is given by

$$v = v_c \sin\psi , \qquad (11)$$

where v_c is the (horizontal) cruising velocity. The v caused the Doppler shift f_d given by Eq. (6). The relationship between ψ

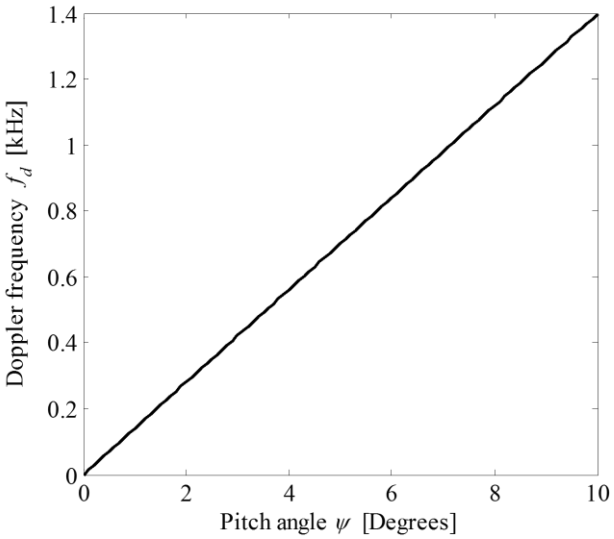

Fig. 14. Relationship between the pitch direction and the Doppler frequency.

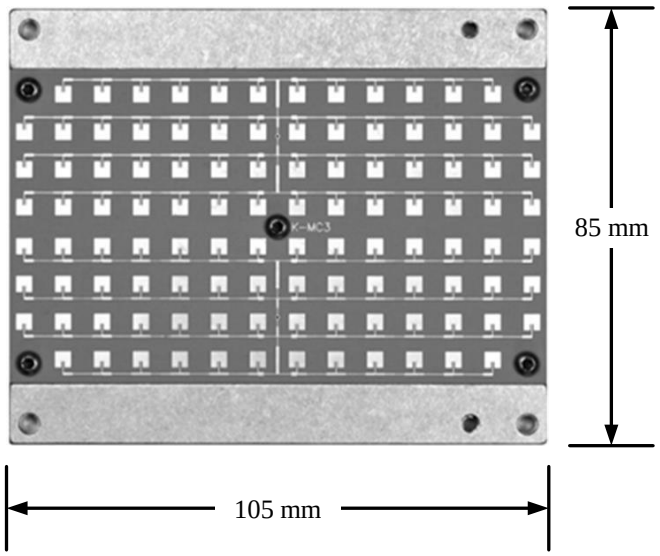

Fig. 15. Antennas for transmission (upper half) and reception (lower half) (the scall is 1:1.5)[6].

and f_d is presented in Fig. 14, which reveals that $f_d << f_b$.

V. Prototyping the Radar Altimeter

A breadboard model was constructed comprising commercially available short range FM-CW radar and other integrated circuit, listed in Tables III, IV, and V. This radar included the transmitting and receiving antennas and RF circuits, and weighed 102g. The sampling rate of the ADC was set at 400 kS/s to suppress its power consumption. The microprocessor was operated at a clock frequency of 72 MHz and a data length of 32 bits. The triangular waveform generated by a DAC in the micro-controller was led into the modulation signal input on the radar.

TABLE III
THE SPECIFICATION OF THE RADAR[6]

Manufacture	RFbeam Microwave GmbH	
Model	K-MC3	
Power supply	5	V
Current	80	mA
Transmitting power	19	dBm
Antenna gain	21	dBi
Center frequency	24.15	GHz
VCO sensitivity	22	MHz/V
Receiver sensitivity	-126	dBm

TABLE IV
THE SPECIFICATION OF THE ADC[7]

Manufacture	Analog Devices Inc.	
Model	ADC7671	
Power supply	5	V
Maximum sampling rate	1	MSps
Number of bits	16	bit
Imputable voltage(unipolar)	0 – 5	V
Interface	Parallel	
Power consumption	15	μW @ 100 Sps

TABLE V
THE SPECIFICATION OF THE MICRO-CONTROLLER[8]

Manufacture	NXP Semiconductors Inc.	
Model	LPC2388	
Power supply	3.3	V
Maximum clock frequency	72	MHz
Flash	512	kB
SRAM	64	kB
Number of bits of DAC	10	bit

VI. Experimental Evaluation

A. Measurement Setup

An outdoor experiment was carried out by using a vertical concrete wall as an extended target. The transmitting and receiving antennas (Fig. 15) were placed at a height of 1.4 m above the ground. The antenna beam was horizontal and perpendicular to the wall. Clutter from the ground and other structures were negligibly small. The frequency excursion Δf = 200 MHz, the frequency of the triangular waveform f_m = 1 kHz, and the measurement range R was from 5 to 24 m in this experiment. From Eq. (3), f_b was found to be 64 kHz when R = 24 m, but in reality f_b was approximately 70 kHz in consideration of the delay within the feeding coaxial cables. From Eq. (8), the resolution of range was 0.09 m.

B. Measurement Results

An example of the FFT output when R = 10 m is depicted in Fig. 16. The FFT result in Fig. 16 (a) included spurious at approximately 4 kHz caused by coupling between transmitting and receiving antennas, which resulted in false estimation of range. A high pass filter having a cutoff frequency of 15 kHz

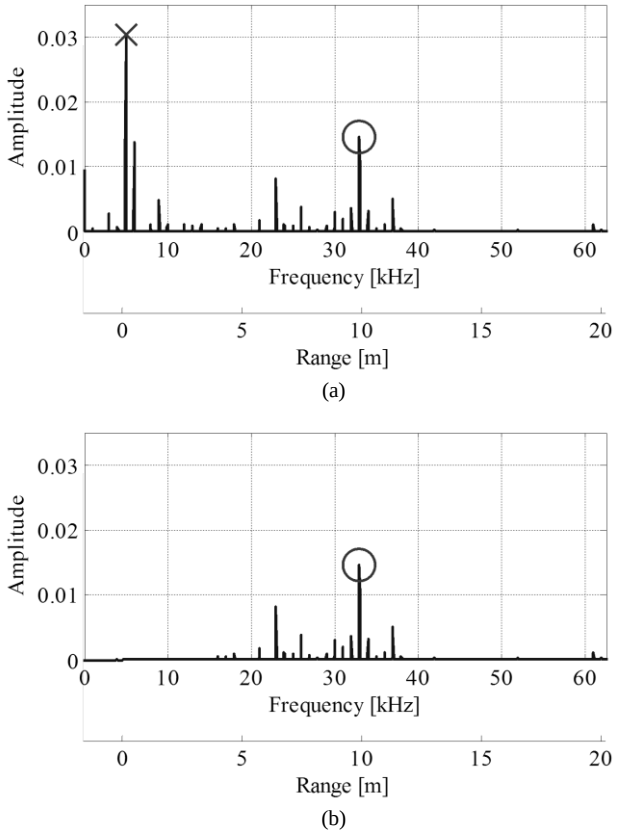

Fig. 16. Examples of spectra of the beat signals measured when R = 10 m: (a)containing spurious peak (denoted by "×") caused by coupling between the transmitter to the receiver and (b) the coupling was suppressed with use of a high-pass filter.

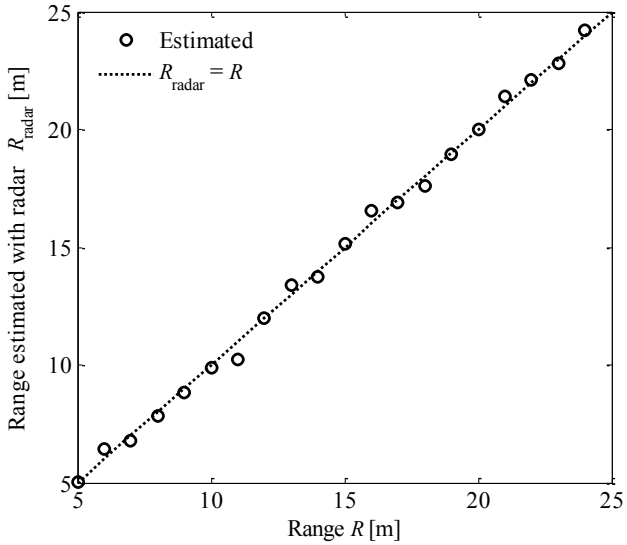

Fig. 17. The relationship between the range and that estimated with radar.

was applied to the beat signal to suppress the spurious, as shown in Fig. 16 (b). The resulting FFT spectrum yielded a correct estimation of R = 10 m. The relationship between the range measured with a tape measure and that estimated with the radar is presented in Fig. 17. The standard deviation of the radar estimation was 0.31 m.

VII. Conclusion

This paper presents a feasibility study of the radar altimeter for an UAV cruising in the Mars' atmosphere. Feasibility of the altimeter was examined within limits of weight and power consumption through the adoption of a FM-CW radar technology. To estimate the achievable SNR, the normalized radar cross section of the Mars' surface was extrapolated from the past radar observation of the earth and the moon. Link budget estimation based on the radar equation revealed that the altitude can be reliably measured under the severest conditions at an altitude of 10 km.

Preliminary experimental evaluation was carried out with use of a breadboard model against vertical concrete wall. Good agreement was observed between the real range (measured with a tape measure) and that estimated with the radar. An unmanned helicopter experiment will be carried out to extend the range.

References

[1] T. Kubota *et al.*, "Preliminary study on lander system and scientific investigation for next Mars exploration," ISTS2009-K-21, *27th International Symposium on Space Technology and Science* (*ISTS 2009*), Tsukuba, Japan, Jul. 2009.

[2] H. Nagai, A. Oyama, and Mars Airplane WG, "Mission scenario of Mars exploration by airplane," *The 2013 Asia-Pacific International Symposium on Aerospace Technology* , Takamatsu, Japan, Nov. 2013.

[3] T. Tagawa *et al.*, "Measurement of scattering coefficients of soil by Ka-band polarimetric scatteromter−dependence on soil moisture content and surface roughness−," *IEICE Trans. Commun.* (in Japanese), vol. J89-B, no. 2 pp. 286-295, Feb. 2006.

[4] B. A. Campbell, "*Radar Remote Sensing of Planetary Surface*," Cambridge Univ. Press, Cambridge, 2002.

[5] H. Tokutake *et al*., "Attitude sensing system using photodetectors," *International Workshop on Instruction for Planetary Missions*, Greenbelt, MD, no. 1683, pp. 1022-1024, Oct. 2012

[6] RFbeam Microwave GmbH, "K-MC3 RADAR TRANSCEIVER Datasheet," http://www.rfbeam.ch/, May 2011.

[7] Analog Devices Inc., "AD7671 Data-sheet," http://www.analog.com, Jul 2005.

[8] NXP Semiconductors, "LPC23XX User manual," http://www.nxp.com/, Aug 2011.

Sho Yonemura received the B.E. degree in information and communication engineering at Tokyo Denki University in 2012. He is currently pursuing the M.E. degree at the same university. His research interests radar signal processing.

Atsushi Tomiki received B.E., M.E., and Ph.D. degrees from Tokyo Denki University in 2002, 2004, and 2007, respectively. He joined the Japan Aerospace Exploration Agency (JAXA), Sagamihara, Japan in 2007 and was engaged in development of deep space communication systems. He is currently an assistant professor at the Department of Spacecraft Engineering, the Institute of Space and Astronautical Science in JAXA. His research interests include

UWB systems for fly-by-wireless, and electromagnetic compatibility in scientific spacecrafts.

Tomoaki Toda received the B.S., M.S., and Ph.D. degrees in electronic engineering from the University of Tokyo, Tokyo, Japan, in 1994, 1996, and 1999, respectively. Since 1999, he has been with the Institute of Space and Astronautical Science, Sagamihara, Japan and responsible for RF and optical telecommunication technologies of space exploration missions of the institute. His current research interests are in deep space communication systems using RF and optical signals and applications of wireless technologies for the innovation of spacecraft design.

Takehiko Kobayashi received the B.E., M.E., and Ph.D. degrees in electrical engineering from the University of Tokyo in 1978, 1980, and 1983. He joined Nippon Telegraph and Telephone in 1983 and was engaged in research on various wireless communication systems. He was a guest scientist at National Bureau of Standard (now NIST) in Boulder, Colorado, U. S. A. from 1986 to 1987. From 1998 to 2001, he was with YRP Key Tech Labs, which focused on the 4th generation mobile communication systems. Currently, he is a professor at the Department of Information and Communication Engineering, Tokyo Denki University. He received the IEICE Best Paper Awards in 2001 and 2002, the IEICE Achievement Award in 2008, and the Telecom System Awards from the Telecommunications Advancement Foundation in 2003 and 2005. His current research interests include ultra wideband wireless systems, mobile communication channel characterization, and teletraffic evaluation of mobile communication networks.